Measurement of the Ratios of Branching Fractions $\mathcal{R}(D^*)$ and $\mathcal{R}(D^0)$

R. Aaij *et al.*[*]
(LHCb Collaboration)

(Received 9 February 2023; revised 18 April 2023; accepted 29 June 2023; published 13 September 2023)

The ratios of branching fractions $\mathcal{R}(D^*) \equiv \mathcal{B}(\bar{B} \to D^* \tau^- \bar{\nu}_\tau)/\mathcal{B}(\bar{B} \to D^* \mu^- \bar{\nu}_\mu)$ and $\mathcal{R}(D^0) \equiv \mathcal{B}(B^- \to D^0 \tau^- \bar{\nu}_\tau)/\mathcal{B}(B^- \to D^0 \mu^- \bar{\nu}_\mu)$ are measured, assuming isospin symmetry, using a sample of proton-proton collision data corresponding to 3.0 fb^{-1} of integrated luminosity recorded by the LHCb experiment during 2011 and 2012. The tau lepton is identified in the decay mode $\tau^- \to \mu^- \nu_\tau \bar{\nu}_\mu$. The measured values are $\mathcal{R}(D^*) = 0.281 \pm 0.018 \pm 0.024$ and $\mathcal{R}(D^0) = 0.441 \pm 0.060 \pm 0.066$, where the first uncertainty is statistical and the second is systematic. The correlation between these measurements is $\rho = -0.43$. The results are consistent with the current average of these quantities and are at a combined 1.9 standard deviations from the predictions based on lepton flavor universality in the standard model.

DOI: 10.1103/PhysRevLett.131.111802

Semileptonic b hadron decays provide a powerful laboratory for testing the equality of the couplings of the three charged leptons to the gauge bosons, a fundamental characteristic of the standard model (SM), known as lepton flavor universality (LFU). Measurements of the LFU-sensitive ratios of branching fractions $\mathcal{R}(D^*) \equiv \mathcal{B}(\bar{B} \to D^* \tau^- \bar{\nu}_\tau)/\mathcal{B}(\bar{B} \to D^* \ell^- \bar{\nu}_\ell)$, where D^* indicates either D^{*+} or D^{*0} and ℓ indicates a light lepton (the inclusion of charge-conjugate processes is implied throughout this Letter), $\mathcal{R}(D) \equiv \mathcal{B}(\bar{B} \to D \tau^- \bar{\nu}_\tau)/\mathcal{B}(\bar{B} \to D \ell^- \bar{\nu}_\ell)$ [1–7], where D indicates D^+ or D^0, and $\mathcal{R}(J/\psi) \equiv \mathcal{B}(B_c^- \to J/\psi \tau^- \bar{\nu}_\tau)/\mathcal{B}(B_c^- \to J/\psi \mu^- \bar{\nu}_\mu)$ [8] show an excess of semitauonic decays over the SM predictions, whereas a measurement of $\mathcal{R}(\Lambda_c^+) \equiv \mathcal{B}(\Lambda_b^0 \to \Lambda_c^+ \tau^- \bar{\nu}_\tau)/\mathcal{B}(\Lambda_b^0 \to \Lambda_c^+ \mu^- \bar{\nu}_\mu)$ [9] is found to be consistent with the SM. A summary of predictions of $\mathcal{R}(D)$ and $\mathcal{R}(D^*)$ in particular is presented in Table I.

The LHCb Collaboration has previously reported on LFU studies in the $b \to c$ semileptonic decays using the data recorded during 2011–2012: two measurements of $\mathcal{R}(D^{*+})$ using the purely leptonic tau decays $\tau^- \to \mu^- \nu_\tau \bar{\nu}_\mu$ [2] and the three-pion decay channel $\tau^- \to \pi^- \pi^+ \pi^- (\pi^0) \nu_\tau$ [5,6], as well as measurements of the observables $\mathcal{R}(J/\psi)$ in the leptonic channel [8] and $\mathcal{R}(\Lambda_c^+)$ in the three-pion channel [9]. This Letter presents the first simultaneous measurement of $\mathcal{R}(D^*)$ and $\mathcal{R}(D^0)$ in hadron collisions, and supersedes the result of Ref. [2]. The data correspond to integrated luminosities of 1.0 fb^{-1} and 2.0 fb^{-1}, collected by the LHCb detector in proton-proton collisions with center-of-mass energies of 7 TeV and 8 TeV, respectively. Owing to the different spin structures of the $\bar{B} \to D^* \ell^- \bar{\nu}_\ell$ and $\bar{B} \to D \ell^- \bar{\nu}_\ell$ decays, the combined result provides significantly improved sensitivity to the structure of possible LFU-breaking processes originating from physics beyond the SM, such as the effects of an extended Higgs mechanism or leptoquarks (see, e.g., the recent review in Ref. [20]).

This study utilizes the purely leptonic tau decay $\tau^- \to \mu^- \nu_\tau \bar{\nu}_\mu$ for the reconstruction of the semitauonic $\bar{B} \to D^{(*)} \tau^- \bar{\nu}_\tau$ decays, where $D^{(*)}$ stands for a D^0, a D^{*+}, or a D^{*0} meson. These decays, hereafter denoted as the signal channels, as well as $\bar{B} \to D^{(*)} \mu^- \bar{\nu}_\mu$ decays, which serve as the normalization for the determination of the $\mathcal{R}(D^0)$ and $\mathcal{R}(D^*)$ observables, are identified using the

TABLE I. Summary of calculations of $\mathcal{R}(D)$ and $\mathcal{R}(D^*)$ as compiled by the HFLAV collaboration [10]. For consistency with HFLAV this Letter uses the same average value $\mathcal{R}(D) = 0.298 \pm 0.004$, $\mathcal{R}(D^*) = 0.254 \pm 0.005$ when making comparisons with the standard model.

$\mathcal{R}(D)$	$\mathcal{R}(D^*)$	Reference
0.299 ± 0.003	...	[11]
...	$0.254^{+0.007}_{-0.006}$	[12]
0.298 ± 0.003	0.247 ± 0.006	[13]
0.299 ± 0.003	0.257 ± 0.003	[14]
0.299 ± 0.004	0.257 ± 0.005	[15]
...	0.253 ± 0.005	[16]
0.296 ± 0.008	...	[17]
...	0.260 ± 0.008	[18]
...	0.265 ± 0.013	[19]

[*]Full author list given at the end of the Letter.

visible final states $D^0\mu^-$ and $D^{*+}\ \mu^-$. Both signal and normalization channels are selected by a common reconstruction procedure, which selects events containing a muon candidate and a $D^0 \to K^-\pi^+$ candidate with the expected flavor correlation, $D^0\mu^-$, from $b \to c$ semileptonic decays. The sample is divided into $D^0\mu^-$ and $D^{*+}\ \mu^-$ samples according to whether the combination of the D^0 with any track in the event forms a D^{*+} candidate with a mass difference $\Delta m < 160\ \mathrm{MeV}/c^2$, where Δm is the difference between the D^{*+} and D^0 candidate masses.

The $D^0\mu^-$ sample contains contributions from $B^- \to D^0\tau^-\bar{\nu}_\tau$ and $B^- \to D^0\mu^-\bar{\nu}_\mu$ decays as well as contributions from partially reconstructed $B^- \to D^{*0}\mu^-\bar{\nu}_\mu$, $\bar{B}^0 \to D^{*+}\mu^-\bar{\nu}_\mu$, $B^- \to D^{*0}\tau^-\bar{\nu}_\tau$, and $\bar{B}^0 \to D^{*+}\tau^-\bar{\nu}_\tau$ decays through the decay chains $D^{*+} \to D^0\pi^+$, $D^{*0} \to D^0\gamma$, and $D^{*0} \to D^0\pi^0$, where the photon or pion is not reconstructed. The $D^{*+}\mu^-$ candidate sample, which contains $\bar{B}^0 \to D^{*+}\tau^-\bar{\nu}_\tau$ and $\bar{B}^0 \to D^{*+}\mu^-\bar{\nu}_\mu$ and no substantial contribution from the other signal or normalization decays, was the basis of the first measurement of $\mathcal{R}(D^*)$ by the LHCb Collaboration [2]. The simultaneous analysis of the two samples helps to constrain the common parameters of the fit models that are applied to the data, reducing the correlation between the measured values of $\mathcal{R}(D^0)$ and $\mathcal{R}(D^*)$.

In addition to the signal and the normalization channels, the selected samples contain contributions from several background processes, which include partially reconstructed B decays, such as semileptonic decays with an excited charmed meson and hadronic B decays into two charmed mesons, with one of them decaying (semi)leptonically; cases where the muon candidate originates from the misidentification of other charged particles; and combinations of unrelated particles from different decay chains. The kinematic and the topological properties of the various components are exploited to suppress background contributions. The relative contributions of the processes present in the data samples are determined by fitting to the data a model composed of multidimensional template distributions derived from control samples in data or from simulation validated against data.

The LHCb detector, described in detail in Refs. [21,22], is a single-arm forward spectrometer covering the pseudorapidity range $2 < \eta < 5$, designed for the study of particles containing b or c quarks. The online event selection is performed by a trigger [23], which consists of a hardware stage, based on information from the calorimeter and muon systems, followed by a software stage, which applies a full event reconstruction. Simulation produced by software packages described in Refs. [24–29] is used to model the physics processes and the effects of both the detector acceptance and the selection criteria.

The events are required to pass the hardware trigger independently of the muon candidate, as the requirement in the hardware trigger on the component of the muon momentum transverse to the beam, $p_T(\mu)$, would significantly reduce the selection efficiency of the semitauonic decays. Therefore, the events must pass the hardware trigger either because the decay products of the $D^0 \to K^-\pi^+$ candidate satisfy the hadron trigger requirements or because unrelated high-p_T particles in the event satisfy any of the hardware trigger requirements. In the software trigger, the events are required to meet criteria designed to accept $D^0 \to K^-\pi^+$ candidates with $p_T > 2\ \mathrm{GeV}/c$. Quality requirements are applied to the tracks of the charged particles that originate from a candidate D^0 decay: their momenta must exceed 5 GeV/c, and at least one track must have $p_T > 1.5\ \mathrm{GeV}/c$. The momentum vector of the D^0 candidate must align approximately with the displacement from one of the primary vertices (PV) in the event, and the reconstructed mass must be consistent with the known D^0 mass [30].

In the offline reconstruction, K^- and π^+ candidates from the D^0 decay are required to satisfy loose particle identification requirements, and the decay vertex is required to be significantly displaced from all PVs. The invariant mass of the D^0 candidate is required to be consistent with the D^0 mass within 3 times the resolution, as determined by a fit to data. The muon candidate is required to be consistent with a muon signature in the detector, to have momentum $3 < p < 100\ \mathrm{GeV}/c$, to be significantly separated from any PV, and to form a good vertex with the D^0 candidate. To reduce further the background from hadrons misidentified as muons ("misID background"), muon likelihood-ratio identification criteria used previously [2] are supplemented with a dedicated multivariate selector, trained on information from multiple subdetectors, constrained to provide uniform efficiency in muon momentum and p_T using the uBoost method [31]. The $D^0\mu^-$ combinations are required to have an invariant mass less than 5280 MeV/c^2, and their momentum vector is required to align approximately with the displacement vector from the associated PV to the $D^0\ \mu^-$ vertex, which removes random combinations while preserving a large fraction of semileptonic decays. In addition to the signal candidates, independent samples of "wrong sign" candidates, $D^0\mu^+$, $D^{*+}\mu^+$, and $D^0\pi^-\mu^-$, are selected for estimating the combinatorial background. The first two represent random combinations of $D^{(*)}$ candidates with muons from unrelated decays, and the latter is used to model the contribution of misreconstructed D^{*+} decays. The background from misreconstructed $D^0 \to K^-\pi^+$ candidates is negligible. Mass regions $5.28 < m(D^0\mu^-) < 10\ \mathrm{GeV}/c^2$ and $\Delta m < 160\ \mathrm{MeV}/c^2$ are included in all samples to study the combinatorial backgrounds.

To suppress the contributions from partially reconstructed B decays, the signal candidates are required to be isolated from additional tracks in the event. The isolation algorithm is described in Ref. [2]. Except for the muon identification procedure, the selection criteria for the $D^{*+}\mu^-$ sample are unchanged from those used in Ref. [2].

Kinematic variables in the B candidate rest frame, approximated from the laboratory quantities by taking the B boost along the beam axis to be equal to that of the visible candidate [2], are used to characterize and discriminate between the various processes. These variables are the muon energy in the B rest frame, E^*_μ; the missing mass squared, defined as $m^2_{\text{miss}} = (p_B - p_{D^{(*)}} - p_\mu)^2$; and the squared four-momentum transfer to the lepton system, $q^2 = (p_B - p_{D^{(*)}})^2$, where p_B, $p_{D^{(*)}}$ and p_μ are the four-momenta of the B meson, the D^0 (or D^{*+}) meson and the muon.

Simulated events are used to derive the distributions of the B candidate rest-frame kinematic variables for the signal and the normalization channels as well as background from other partially reconstructed b hadron decays. The sum of these multidimensional template distributions, which depends on shape parameters and the relative yields of the contributing processes, forms the fit model applied to the data. Two independent fit model implementations and associated frameworks using common form-factor and correction parametrizations have been developed and applied to the data allowing for cross checks on nearly all aspects of the analysis.

The simulated samples of $\bar{B} \to D^*\mu^-\bar{\nu}_\mu$ and $\bar{B} \to D^*\tau^-\bar{\nu}_\tau$ decays are weighted to the Boyd, Grinstein, and Lebed (BGL) form-factor parametrization [32] using values presented in Refs. [11,15,18] as a starting point. For the decays $B^- \to D^0\mu^-\bar{\nu}_\mu$ and $B^- \to D^0\tau^-\bar{\nu}_\tau$, form factors are described using the parametrization of Refs. [33,34]. For the results presented here, the BGL form-factor expansion coefficients up to order z^2 are allowed to vary in the fit with loose likelihood constraints only for those describing the helicity-suppressed form factors.

The backgrounds from semileptonic $\bar{B}$ decays to the lowest-lying excited charm states $D_1(2420)$, $D_2^*(2460)$, $D_1'(2430)$, and $D_0^*(2300)$ (collectively referred to as D^{**}) are weighted to the form-factor parametrization presented in Ref. [35]. These form-factor parameters, which are allowed to vary without constraint in the fit, are constrained by control regions in the data, described below. Background from $\bar{B}_s^0$ decays to the states $D_{s1}(2536)^+$ and $D_{s2}^*(2573)^+$, (together denoted as D_s^{**}) which subsequently decay as $D_s^{**+} \to D^{*+}K^0$ or $D_s^{**+} \to D^0K^+$, are modeled using the same form-factor parametrization, with values unconstrained and independent of those for the D^{**} states. Backgrounds from semileptonic B decays to heavier excited charm states D^{**}_{heavy} decaying as $D^{**}_{\text{heavy}} \to D^{(*)}\pi\pi$ are modeled using simulated samples containing a mix of final states generated with the ISGW2 [36] form factors. As the composition and decay properties of this background are not well understood, an *ad hoc* weight is applied as a linear function of the true q^2 with independent slopes for decays to D^{*+}, D^{*0}, and D^0, which vary in the fit and are constrained by control regions in the data.

For the background from B decays into two charmed mesons, simulated samples of $\bar{B}^0$ and B^- decays $B \to D^{*+}H_cX$ and $B \to D^0H_cX$ with a mix of final states are used, where H_c is a charm meson that decays (semi)leptonically, yielding a correct-sign secondary muon to combine with the D^0 or D^{*+}, and X is any combination of light hadrons (e.g., a K or K^* meson). The multibody decays are simulated uniformly in phase space. Control samples (discussed below) are included to constrain corrections applied to the decay distribution. The corrections involve weights given by linear and quadratic functions of the invariant mass of the two primary charm hadrons as well as variations of the size of the contribution of modes with $m(X) > 680$ MeV$/c^2$, where the additional particles X are mostly K^* resonances. A separate sample is used to model the contribution from tertiary muons from $H_c = D_s^{[*(*)]-}$ with the leptonic decay $D_s^- \to \tau^-\bar{\nu}_\tau$.

To model the contribution of misID background, a control sample of D^0 or D^{*+} candidates paired with a single track is used, where the combinations pass all the analysis selection criteria but the single track has no associated segment in the muon system. The two fit models employ two different techniques to produce a model of the misidentified backgrounds by weighting this control sample. Both techniques produce per-track weights using particle identification classification information on the extra track, π, K, p, or e, or unidentified, combined with particle identification efficiencies from large calibration samples. Details are given in the Supplemental Material [37]. Both techniques are independently validated by fitting data samples in which the muon candidate passes initial muon identification criteria, but fails to pass the custom multivariate muon identification developed for this analysis.

Combinatorial backgrounds are classified based on whether or not a genuine $D^{*+} \to D^0\pi^+$ decay is present. Wrong-sign $D^0\pi^-\mu^-$ combinations are used to determine the component with misreconstructed D^{*+} candidates. The size of this contribution is constrained by a fit to the Δm distribution of $D^{*+}\mu^-$ candidates. The contribution from correctly reconstructed D^{*+} candidates combined with μ^- from unrelated b hadron decays is determined from wrong-sign $D^{(*)}\mu^+$ combinations. In both cases, the contributions of misidentified muons are subtracted when generating the kinematic distributions for the fit. The mass region $5.28 < m(D^{(*)}\mu^\mp) < 10$ GeV$/c^2$ excludes genuine B decays, and is used to validate the agreement between the kinematic distributions for wrong-sign and correct-sign combinatorial background candidates.

Extensive studies are performed to account for differences between the data and the simulation. An initial set of corrections to the b hadron production distributions is applied based on weights derived from the comparison of a sample of reconstructed $B^+ \to J/\psi K^+$ decays in data and simulation. A sequence of additional corrections, as a function of kinematic and topological variables, is then applied to the simulation using a control sample of $D^0\mu^-$ candidates with $m^2_{\rm miss} < 0.4\ {\rm GeV}^2/c^4$, which is dominated by the $\bar{B} \to D^{(*)}\mu^-\bar{\nu}_\mu$ decay. Further corrections are applied using the corresponding region of the $D^{*+}\mu^-$ sample to correct residual differences between data and simulation in the reconstruction of the low-momentum π^+ in the $D^{*+} \to D^0\pi^+$ decay. The combined correction results in an rms bin-by-bin change to the fit templates on the order of 3%, and improves the modeling of both the acceptance and the resolution for the fit variables (and therefore bin migration effects), including correlations. This procedure is, in principle, iterative, but converges after a single round of corrections, and residual differences are covered in the systematic uncertainties discussed below.

In order to constrain the modeling of the various backgrounds presented above, several control regions enhanced in the background contributions are selected in both the $D^0\mu^-$ and $D^{*+}\mu^-$ data based on the output of the isolation algorithm. Requiring the presence of a charged kaon candidate among the particles accompanying the $D^{(0,*+)}\mu^-$ candidate results in a sample with an enhanced fraction of B decays into two charmed mesons. Samples enriched in semileptonic B decays to D^{**} are selected by requiring the presence of exactly one additional pion candidate in the vicinity of the $D^{(0,*+)}\mu^-$ candidate with the correct relative charge for the $D^{**} \to D^{(*)}\pi$ decay. Requiring exactly two accompanying pion candidates of opposite charge provides a sample with enhanced fraction of decays to $D^{**}_{\rm heavy}$ mesons. The three isolation output selections above, selected in both $D^0\mu^-$ and $D^{*+}\mu^-$ samples, constitute six distinct control regions. Including the isolated $D^0\mu^-$ and $D^{*+}\mu^-$ signal region, eight regions are selected in total for the fit.

The binned distributions of $m^2_{\rm miss}$ ($[-2, 10.6]\ {\rm GeV}^2/c^4$, 43 bins), E^*_μ ([100, 2650] MeV, 34 bins), and q^2 ($[-0.4, 12.6]\ {\rm GeV}^2/c^4$, four bins) for reconstructed $D^0\mu^-$ and $D^{*+}\mu^-$ candidates in data are fit using a binned extended maximum-likelihood method with three-dimensional templates representing the signal and normalization channels and the background sources. The model parameters extracted from the data include the yields of each contributing process: signals, normalizations, $\bar{B} \to D^{**}\ell^-\bar{\nu}_\ell$ (with a Gaussian-constrained fraction of $\bar{B} \to D^{**}\tau^-\bar{\nu}_\tau$), $\bar{B} \to D^{**}_{\rm heavy}\mu^-\bar{\nu}_\mu$, $\bar{B}^0_s \to D^{**}_s\mu^-\bar{\nu}_\mu$, $\bar{B} \to D^{*+}H_c(\to \mu^-\bar{\nu}_\mu X')X$ (with a Gaussian-constrained fraction of $\bar{B} \to D^{(*)}D^-_s(\to \tau^-\bar{\nu}_\tau)X$), misID background, and combinatorial backgrounds. The form-factor parameters for signal, normalization, and $D^{**}_{(s)}$ backgrounds are allowed to vary in the fit, as is the level of momentum smearing applied to the misID component to account for kaon or pion decays to muons. The same fit model is applied to all selected regions with appropriately selected templates, with form-factor parameters and shape correction parameters shared between regions, and yield parameters allowed to vary independently by region. Statistical uncertainties in the templates are folded into the likelihood via the Beeston-Barlow "lite" prescription [41]. Projections of the fit in each control region are shown in the Supplemental Material [37].

Two approaches are used to incorporate the information from the control regions. For the result presented here, all eight regions are fit simultaneously using a custom likelihood implementation in the ROOT [42] software package to extract $\mathcal{R}(D^0)$ and $\mathcal{R}(D^*)$ including all correlations. In the alternative fit, built using the RooFit [43] and HistFactory [44] frameworks, the six control regions are fit simultaneously first to obtain corrections to the most signal-like backgrounds in signal-depleted regions. The two signal samples are then fit with shapes fixed (or likelihood-constrained in the case of the $\bar{B} \to D^{**}\mu^-\bar{\nu}_\mu$ and $\bar{B}^0_s \to D^{**}_s\mu^-\bar{\nu}_\mu$ form-factor parameters) according to the result of the control fit. The two fitters have been extensively cross-validated and give consistent results within an expected statistical spread determined using common pseudodatasets. As the two results are compatible, only the results of the former fit are presented in this Letter.

The results of the fit to the isolated (signal) samples are shown in Fig. 1. The complete set of projections for all q^2 bins can be found in the Supplemental Material [37]. The ratios of branching fractions are determined to be $\mathcal{R}(D^0) = 0.441 \pm 0.060$, $\mathcal{R}(D^*) = 0.281 \pm 0.018$, with a correlation $\rho = -0.49$, where the statistical uncertainties are evaluated with all nuisance parameters related to template shape uncertainties fixed to their respective best-fit values. The obtained yields of normalization (signal) are 324 000 (12 000) $\bar{B}^0 \to D^{*+}l^-\bar{\nu}_l$ decays in the $D^{*+}\mu^-$ signal sample, and 354 000 (20 000) $B^- \to D^0 l^-\bar{\nu}_l$ decays, 958 000 (34 000) $B^- \to D^{*0}l^-\bar{\nu}_l$ decays, and 44 000 (1 700) $\bar{B}^0 \to D^{*+}l^-\bar{\nu}_l$ decays in the $D^0\mu^-$ sample, where $l = \mu$ (τ). The $\bar{B}^0 \to D^{*+}\mu^-\bar{\nu}_\mu$ yield in the $D^{*+}\mu^-$ sample is consistent with the previous measurement [2] after accounting for the efficiency of the stricter muon identification criteria used here.

Uncertainties in the measurements of $\mathcal{R}(D^0)$ and $\mathcal{R}(D^*)$ are summarized in Table II. The uncertainty in extracting $\mathcal{R}(D^{(*)})$ from the fit (model uncertainty) is dominated by the statistical uncertainty of the simulated samples; this contribution is estimated via the reduction in the fit uncertainty when the template statistical uncertainty is not considered in the likelihood. Form-factor parameters are included in the likelihood as nuisance parameters; hence the associated systematic uncertainties are contained in the total uncertainties of $\mathcal{R}(D^0)$ and $\mathcal{R}(D^*)$ determined with all nuisance parameters allowed to vary. To determine

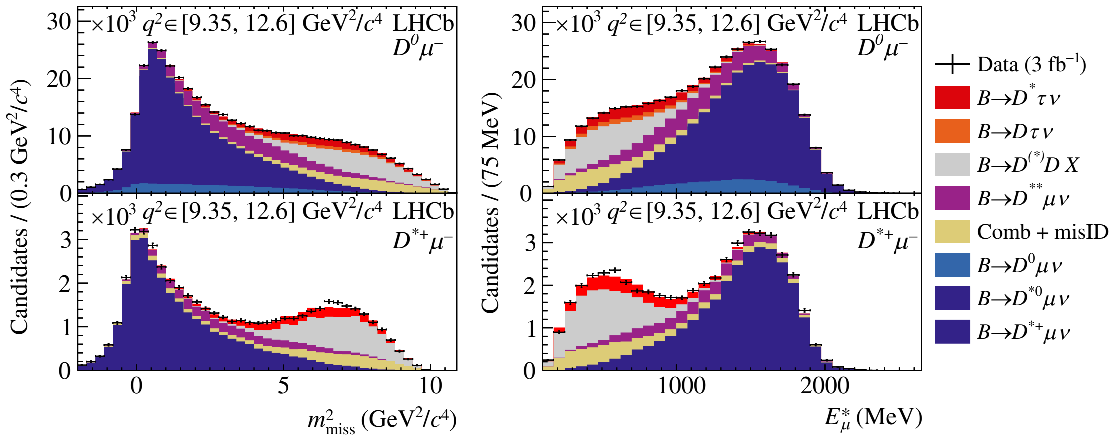

FIG. 1. Distributions of (left) $m^2_{\rm miss}$ and (right) E^*_μ in the highest q^2 bin (above 9.35 GeV^2/c^4) of the (top) $D^0\,\mu^-$ and (bottom) $D^{*+}\,\mu^-$ signal data, overlaid with projections of the fit model.

the contribution of the form-factor uncertainty, the fit is repeated with form-factor parameters fixed to their best-fit values, and the reduction in uncertainty compared with the configuration with varying nuisance parameters is used to determine the contribution from the form-factor uncertainties. The systematic uncertainty from empirical corrections to the kinematic distributions of $\bar{B}\to D^{**}(\to D^{(*)}\pi\pi)\mu^-\bar{\nu}_\mu$ and $\bar{B}\to D^{(*)}H_c(\to \mu\nu_\mu X')X$ backgrounds is computed in the same way.

The contribution of $B\to D^{**}_{(s)}\tau^-\bar{\nu}_\tau$ decays relative to $B\to D^{**}_{(s)}\mu^-\bar{\nu}_\mu$ is likelihood constrained to an expectation of 8% taken from Ref. [35], with a relative uncertainty of 30% assigned to cover both the inclusion of different $D^{**}_{(s)}\tau^-\bar{\nu}_\tau$ states, and the possibility of LFU violation in

TABLE II. Absolute uncertainties in the extraction of $\mathcal{R}(D^0)$ and $\mathcal{R}(D^*)$. The model uncertainties are divided into those included directly in the fit likelihood and those determined via supplemental studies.

Internal fit uncertainties	$\sigma_{\mathcal{R}(D^*)}$ $(\times 10^{-2})$	$\sigma_{\mathcal{R}(D^0)}$ $(\times 10^{-2})$	Correlation
Statistical uncertainty	1.8	6.0	−0.49
Simulated sample size	1.5	4.5	
$B\to D^{(*)}DX$ template shape	0.8	3.2	
$\bar{B}\to D^{(*)}\ell^-\bar{\nu}_\ell$ form factors	0.7	2.1	
$\bar{B}\to D^{**}\mu^-\bar{\nu}_\mu$ form factors	0.8	1.2	
$\mathcal{B}\ [\bar{B}\to D^* D_s^-(\to \tau^-\bar{\nu}_\tau)X]$	0.3	1.2	
MisID template	0.1	0.8	
$\mathcal{B}\ (\bar{B}\to D^{**}\tau^-\bar{\nu}_\tau)$	0.5	0.5	
Combinatorial	< 0.1	0.1	
Resolution	< 0.1	0.1	
Additional model uncertainty	$\sigma_{\mathcal{R}(D^*)}$ $(\times 10^{-2})$	$\sigma_{\mathcal{R}(D^0)}$ $(\times 10^{-2})$	
$B\to D^{(*)}DX$ model uncertainty	0.6	0.7	
$\bar{B}^0_s\to D_s^{**}\mu^-\bar{\nu}_\mu$ model uncertainty	0.6	2.4	
Baryonic backgrounds	0.7	1.2	
Coulomb correction to $\mathcal{R}(D^{*+})/\mathcal{R}(D^{*0})$	0.2	0.3	
Data-simulation corrections	0.4	0.8	
MisID template unfolding	0.7	1.2	
Normalization uncertainties	$\sigma_{\mathcal{R}(D^*)}$ $(\times 10^{-2})$	$\sigma_{\mathcal{R}(D^0)}$ $(\times 10^{-2})$	
Data-simulation corrections	$0.4\times\mathcal{R}(D^*)$	$0.6\times\mathcal{R}(D^0)$	
$\tau^-\to\mu^-\nu\bar{\nu}$ branching fraction	$0.2\times\mathcal{R}(D^*)$	$0.2\times\mathcal{R}(D^0)$	
Total systematic uncertainty	2.4	6.6	−0.39
Total uncertainty	3.0	8.9	−0.43

these decay modes. Similarly, the contribution of $\bar{B} \to D^{(*)} D_s^- (\to \tau^- \bar{\nu}_\tau) X$ decays is likelihood constrained using known branching fractions [30] with a 30% uncertainty. The systematic uncertainty is again given by the effect of allowing these to vary within the loose 30% constraint versus fixing them to best fit.

The uncertainty in the shape of the misID background due to the limited statistics of control data is determined by allowing the hadron to muon misidentification efficiency vary as a function of lab momentum within the uncertainties from control data and computing the increase in uncertainty in $\mathcal{R}(D^{(*)})$.

The expected yield of $D^{(*)}\mu^-$ candidates compared with $D^{(*)}\mu^+$ candidates (used to model the combinatorial background) varies as a function of $m(D^{(*)}\mu^\mp)$. The size of this effect is estimated in the $5.28 < m(D^{(*)}\mu^\mp) < 10\ \mathrm{GeV}/c^2$ region, and the uncertainty is propagated as a systematic uncertainty in $\mathcal{R}(D^{(*)})$.

The choice of corrections applied to simulated $B \to D^{(*)} H_c X$ decays is not unique, and so the fit is repeated for an ensemble of possible alternative choices. The root mean square of this ensemble is taken as a systematic uncertainty.

A small discrepancy in the fit quality is observed in a region of the control samples dominated by cross feed from $\bar{B}_s^0 \to D_s^{**} \mu^- \bar{\nu}_\mu$ decays. To assess the maximum size of the effect from this mismodeling, a deformation suppressing the low-q^2, low-E_μ^* region of this template to better match the data is applied, and the effect on the signal yield from this change is evaluated.

The default fit model does not include $\Lambda_b^0 \to D^0 p \mu^- \bar{\nu}_\mu$ or $\Lambda_b^0 \to D^{*+} n \mu^- \bar{\nu}_\mu$ decays. To assess the effect of their exclusion, a fit is performed to a control sample requiring a proton candidate among the particles accompanying the $D^0\mu^-$ candidate. The existing $\bar{B} \to D^{**} \mu^- \bar{\nu}_\mu$ simulated samples are reused with different parameter values as proxy for the Λ_b^0 decays and are able to reproduce the kinematic distributions observed in the data. The fit for $\mathcal{R}(D^{(*)})$ is repeated with these components included using one of two possible auxiliary fits to constrain the size of the contribution, and the larger of the two possible shifts of $\mathcal{R}(D^{(*)})$ is assigned as the systematic uncertainty.

The systematic uncertainty due to the absence of the Coulomb interaction in the PHOTOS package [27] is evaluated by weighting the $\bar{B}^0 \to D^{*+} \ell^- \bar{\nu}_\ell$ simulation by the Coulomb factor given in Ref. [45]. It is found that the only significant effect on these results is due to a 1% shift of the expected isospin relationship between $\mathcal{R}(D^{*+})$ and $\mathcal{R}(D^{*0})$, which induces a small shift in $\mathcal{R}(D^0)$ and $\mathcal{R}(D^*)$.

To assess the uncertainty from residual disagreements between data and simulation, a second iteration of the weighting procedure described above is performed using several possible variations of the scheme. Half the largest difference in $\mathcal{R}(D^{(*)})$ is taken as a systematic uncertainty.

The systematic uncertainty from the unfolded kinematic shapes of the misID background is taken to be half the difference from using the two misID determination methods described above.

Uncertainties in converting the fitted ratio of signal and normalization yields into $\mathcal{R}(D^{(*)})$ (normalization uncertainties) primarily come from the uncertainty in the effect of the corrections to simulation and are evaluated similarly. The uncertainty in the current world average value of $\mathcal{B}(\tau^- \to \mu^- \bar{\nu}_\mu \nu_\tau)$ also contributes a small normalization uncertainty.

In conclusion, the branching fraction ratios $\mathcal{B}(\bar{B} \to D^* \tau^- \bar{\nu}_\tau)/\mathcal{B}(\bar{B} \to D^* \mu^- \bar{\nu}_\mu)$ and $\mathcal{B}(B^- \to D^0 \tau^- \bar{\nu}_\tau)/\mathcal{B}(B^- \to D^0 \mu^- \bar{\nu}_\mu)$ are measured to be

$$\mathcal{R}(D^*) = 0.281 \pm 0.018 \pm 0.024$$
$$\mathcal{R}(D^0) = 0.441 \pm 0.060 \pm 0.066$$
$$\rho = -0.43,$$

with ρ the correlation, and where the first uncertainty is statistical and the second is systematic. This is the first measurement of the ratio $\mathcal{R}(D^0)$ at a hadron collider. These results are consistent at less than 1 standard deviation with the current average of these quantities and stand at about 2 standard deviations from the predictions based on lepton flavor universality in the standard model.

We express our gratitude to our colleagues in the CERN accelerator departments for the excellent performance of the LHC. We thank the technical and administrative staff at the LHCb institutes. We acknowledge support from CERN and from the national agencies: CAPES, CNPq, FAPERJ, and FINEP (Brazil); MOST and NSFC (China); CNRS/IN2P3 (France); BMBF, DFG, and MPG (Germany); INFN (Italy); NWO (Netherlands); MNiSW and NCN (Poland); MCID/IFA (Romania); MICINN (Spain); SNSF and SER (Switzerland); NASU (Ukraine); STFC (United Kingdom); DOE NP and NSF (USA). We acknowledge the computing resources that are provided by CERN, IN2P3 (France), KIT and DESY (Germany), INFN (Italy), SURF (Netherlands), PIC (Spain), GridPP (United Kingdom), CSCS (Switzerland), IFIN-HH (Romania), CBPF (Brazil), Polish WLCG (Poland) and NERSC (USA). We are indebted to the communities behind the multiple open-source software packages on which we depend. Individual groups or members have received support from ARC and ARDC (Australia); Minciencias (Colombia); AvH Foundation (Germany); EPLANET, Marie Skłodowska-Curie Actions and ERC (European Union); A*MIDEX, ANR, IPhU and Labex P2IO, and Région Auvergne-Rhône-Alpes (France); Key Research Program of Frontier Sciences of CAS, CAS PIFI, CAS CCEPP, Fundamental Research Funds for the Central Universities, and Sci. & Tech. Program of Guangzhou (China); GVA, XuntaGal, GENCAT, and Prog. Atracción Talento, CM (Spain); SRC (Sweden); the Leverhulme Trust, the Royal Society, and UKRI (United Kingdom).

[1] J. P. Lees *et al.* (*BABAR* Collaboration), Measurement of an excess of $\bar{B} \to D^{(*)}\tau^-\bar{\nu}_\tau$ decays and implications for charged Higgs bosons, Phys. Rev. D **88**, 072012 (2013).

[2] R. Aaij *et al.* (LHCb Collaboration), Measurement of the Ratio of Branching Fractions $\mathcal{B}(\bar{B}^0 \to D^{*+}\tau^-\bar{\nu}_\tau)/\mathcal{B}(\bar{B}^0 \to D^{*+}\mu^-\bar{\nu}_\mu)$, Phys. Rev. Lett. **115**, 111803 (2015); Publisher's Note, Phys. Rev. Lett. **115**, 159901 (2015).

[3] M. Huschle *et al.* (Belle Collaboration), Measurement of the branching ratio of $\bar{B} \to D^{(*)}\tau^-\bar{\nu}_\tau$ relative to $\bar{B} \to D^{(*)}\ell^-\bar{\nu}_\ell$ decays with hadronic tagging at Belle, Phys. Rev. D **92**, 072014 (2015).

[4] S. Hirose *et al.* (Belle Collaboration), Measurement of the τ lepton polarization and $R(D^*)$ in the decay $\bar{B} \to D^*\tau^-\bar{\nu}_\tau$ with one-prong hadronic τ decays at Belle, Phys. Rev. D **97**, 012004 (2018).

[5] R. Aaij *et al.* (LHCb Collaboration), Measurement of the Ratio of the $\mathcal{B}(B^0 \to D^{*-}\tau^+\nu_\tau)$ and $\mathcal{B}(B^0 \to D^{*-}\mu^+\nu_\mu)$ Branching Fractions Using Three-Prong τ-Lepton Decays, Phys. Rev. Lett. **120**, 171802 (2018).

[6] R. Aaij *et al.* (LHCb Collaboration), Test of lepton flavor universality by the measurement of the $B^0 \to D^{*-}\tau^+\nu_\tau$ branching fraction using three-prong τ decays, Phys. Rev. D **97**, 072013 (2018).

[7] G. Caria *et al.* (Belle Collaboration), Measurement of $\mathcal{R}(D)$ and $\mathcal{R}(D^*)$ with a Semileptonic Tagging Method, Phys. Rev. Lett. **124**, 161803 (2020).

[8] R. Aaij *et al.* (LHCb Collaboration), Measurement of the Ratio of Branching Fractions $\mathcal{B}(B_c^+ \to J/\psi\tau^+\nu_\tau)/\mathcal{B}(B_c^+ \to J/\psi\mu^+\nu_\mu)$, Phys. Rev. Lett. **120**, 121801 (2018).

[9] R. Aaij *et al.* (LHCb Collaboration), Observation of the Decay $\Lambda_b^0 \to \Lambda_c^+\tau^-\bar{\nu}_\tau$, Phys. Rev. Lett. **128**, 191803 (2021).

[10] Y. Amhis *et al.*, Averages of b-hadron, c-hadron, and τ-lepton properties as of 2021, Phys. Rev. D **107**, 052008 (2023).

[11] D. Bigi and P. Gambino, Revisiting $B \to D\ell\nu$, Phys. Rev. D **94**, 094008 (2016).

[12] P. Gambino, M. Jung, and S. Schacht, The V_{cb} puzzle: An update, Phys. Lett. B **795**, 386 (2019).

[13] M. Bordone, M. Jung, and D. van Dyk, Theory determination of $\bar{B} \to D^{(*)}\ell^-\bar{\nu}$ form factors at $\mathcal{O}(1/m_c^2)$, Eur. Phys. J. C **80**, 74 (2020).

[14] F. U. Bernlochner, Z. Ligeti, M. Papucci, and D. J. Robinson, Combined analysis of semileptonic B decays to D and D^*: $R(D^{(*)})$, $|V_{cb}|$, and new physics, Phys. Rev. D **95**, 115008 (2017); **97**, 059902(E) (2018).

[15] S. Jaiswal, S. Nandi, and S. K. Patra, Extraction of $|V_{cb}|$ from $B \to D^{(*)}\ell\nu_\ell$ and the standard model predictions of $R(D^{(*)})$, J. High Energy Phys. 12 (2017) 060.

[16] J. P. Lees *et al.* (*BABAR* Collaboration), Extraction of Form Factors from a Four-Dimensional Angular Analysis of $\bar{B} \to D^*\ell^-\bar{\nu}_\ell$, Phys. Rev. Lett. **123**, 091801 (2019).

[17] G. Martinelli, S. Simula, and L. Vittorio, $|V_{cb}|$ and $R(D)^{(*)})$ using lattice QCD and unitarity, Phys. Rev. D **105**, 034503 (2022).

[18] D. Bigi, P. Gambino, and S. Schacht, $R(D^*)$, $|V_{cb}|$, and the heavy quark symmetry relations between form factors, J. High Energy Phys. 11 (2017) 061.

[19] A. Bazavov *et al.* (Fermilab Lattice, MILC, Fermilab Lattice, and MILC Collaborations), Semileptonic form factors for $B \to D^*\ell\nu$ at nonzero recoil from 2 + 1-flavor lattice QCD, Eur. Phys. J. C **82**, 1141 (2022); **83**, 21(E) (2023).

[20] F. U. Bernlochner, M. F. Sevilla, D. J. Robinson, and G. Wormser, Semitauonic b-hadron decays: A lepton flavor universality laboratory, Rev. Mod. Phys. **94**, 015003 (2022).

[21] A. A. Alves Jr. *et al.* (LHCb Collaboration), The LHCb detector at the LHC, J. Instrum. **3**, S08005 (2008).

[22] R. Aaij *et al.* (LHCb Collaboration), LHCb detector performance, Int. J. Mod. Phys. A **30**, 1530022 (2015).

[23] R. Aaij *et al.*, The LHCb trigger and its performance in 2011, J. Instrum. **8**, P04022 (2013).

[24] T. Sjöstrand, S. Mrenna, and P. Skands, PYTHIA 6.4 physics and manual, J. High Energy Phys. 05 (2006) 026.

[25] T. Sjöstrand, S. Mrenna, and P. Skands, A brief introduction to PYTHIA 8.1, Comput. Phys. Commun. **178**, 852 (2008).

[26] D. J. Lange, The EvtGen particle decay simulation package, Nucl. Instrum. Methods Phys. Res., Sect. A **462**, 152 (2001).

[27] P. Golonka and Z. Was, PHOTOS Monte Carlo: A precision tool for QED corrections in Z and W decays, Eur. Phys. J. C **45**, 97 (2006).

[28] J. Allison *et al.* (Geant4 Collaboration), Geant4 developments and applications, IEEE Trans. Nucl. Sci. **53**, 270 (2006).

[29] S. Agostinelli *et al.* (Geant4 Collaboration), Geant4: A simulation toolkit, Nucl. Instrum. Methods Phys. Res., Sect. A **506**, 250 (2003).

[30] R. L. Workman *et al.* (Particle Data Group), Review of particle physics, Prog. Theor. Exp. Phys. **2022**, 083C01 (2022).

[31] J. Stevens and M. Williams, uBoost: A boosting method for producing uniform selection efficiencies from multivariate classifiers, J. Instrum. **8**, P12013 (2013).

[32] C. G. Boyd, B. Grinstein, and R. F. Lebed, Precision corrections to dispersive bounds on form-factors, Phys. Rev. D **56**, 6895 (1997).

[33] H. Na *et al.* (HPQCD Collaboration), $B \to D\ell\nu$ form factors at nonzero recoil and extraction of $|V_{cb}|$, Phys. Rev. D **92**, 054510 (2015).

[34] C. Bourrely, I. Caprini, and L. Lellouch, Model-independent description of $B \to \pi\ell\nu$ decays and a determination of $|V(ub)|$, Phys. Rev. D **79**, 013008 (2009); **82**, 099902(E) (2010).

[35] F. U. Bernlochner and Z. Ligeti, Semileptonic $B_{(s)}$ decays to excited charmed mesons with e, μ, τ and searching for new physics with $R(D^{**})$, Phys. Rev. D **95**, 014022 (2017).

[36] D. Scora and N. Isgur, Semileptonic meson decays in the quark model: An update, Phys. Rev. D **52**, 2783 (1995).

[37] See Supplemental Material at http://link.aps.org/supplemental/10.1103/PhysRevLett.131.111802 for further plots of signal and control regions, as well as a more detailed discussion of the modeling of nonmuon background and a comparison to the previously published result, which includes Refs. [38–40].

[38] M. Pivk and F. R. Le Diberder, sPlot: A statistical tool to unfold data distributions, Nucl. Instrum. Methods Phys. Res., Sect. A **555**, 356 (2005).

[39] *PHYSTAT 2011 Workshop on Statistical Issues Related to Discovery Claims in Search Experiments and Unfolding*,

edited by H. B. Prosper and L. Lyons (CERN, Geneva, 2011), 10.5170/CERN-2011-006.

[40] F. Archilli *et al.*, Performance of the muon identification at LHCb, J. Instrum. **8**, P10020 (2013).

[41] R. J. Barlow and C. Beeston, Fitting using finite Monte Carlo samples, Comput. Phys. Commun. **77**, 219 (1993).

[42] R. Brun and F. Rademakers, ROOT: An object oriented data analysis framework, Nucl. Instrum. Methods Phys. Res., Sect. A **389**, 81 (1997).

[43] W. Verkerke and D. P. Kirkby, The RooFit toolkit for data modeling, eConf C **0303241**, MOLT007 (2003).

[44] K. Cranmer *et al.* (ROOT Collaboration), HistFactory: A tool for creating statistical models for use with RooFit and RooStats, Report No. CERN-OPEN-2012-016, New York University, New York, 2012.

[45] S. Calí, S. Klaver, M. Rotondo, and B. Sciascia, Impacts of radiative corrections on measurements of lepton flavour universality in $B \to D\ell\nu_\ell$ decays, Eur. Phys. J. C **79**, 744 (2019).

R. Aaij,[32] A. S. W. Abdelmotteleb,[50] C. Abellan Beteta,[44] F. Abudinén,[50] T. Ackernley,[54] B. Adeva,[40] M. Adinolfi,[48] P. Adlarson,[77] H. Afsharnia,[9] C. Agapopoulou,[13] C. A. Aidala,[78] Z. Ajaltouni,[9] S. Akar,[59] K. Akiba,[32] P. Albicocco,[23] J. Albrecht,[15] F. Alessio,[42] M. Alexander,[53] A. Alfonso Albero,[39] Z. Aliouche,[56] P. Alvarez Cartelle,[49] R. Amalric,[13] S. Amato,[2] J. L. Amey,[48] Y. Amhis,[11,42] L. An,[42] L. Anderlini,[22] M. Andersson,[44] A. Andreianov,[38] M. Andreotti,[21] D. Andreou,[62] D. Ao,[6] F. Archilli,[31,b] A. Artamonov,[38] M. Artuso,[62] E. Aslanides,[10] M. Atzeni,[44] B. Audurier,[12] I. B Bachiller Perea,[8] S. Bachmann,[17] M. Bachmayer,[43] J. J. Back,[50] A. Bailly-reyre,[13] P. Baladron Rodriguez,[40] V. Balagura,[12] W. Baldini,[21,42] J. Baptista de Souza Leite,[1] M. Barbetti,[22,c] R. J. Barlow,[56] S. Barsuk,[11] W. Barter,[52] M. Bartolini,[49] F. Baryshnikov,[38] J. M. Basels,[14] G. Bassi,[29,d] B. Batsukh,[4] A. Battig,[15] A. Bay,[43] A. Beck,[50] M. Becker,[15] F. Bedeschi,[29] I. B. Bediaga,[1] A. Beiter,[62] S. Belin,[40] V. Bellee,[44] K. Belous,[38] I. Belov,[38] I. Belyaev,[38] G. Benane,[10] G. Bencivenni,[23] E. Ben-Haim,[13] A. Berezhnoy,[38] R. Bernet,[44] S. Bernet Andres,[76] D. Berninghoff,[17] H. C. Bernstein,[62] C. Bertella,[56] A. Bertolin,[28] C. Betancourt,[44] F. Betti,[42] Ia. Bezshyiko,[44] S. Bhasin,[48] J. Bhom,[35] L. Bian,[68] M. S. Bieker,[15] N. V. Biesuz,[21] P. Billoir,[13] A. Biolchini,[32] M. Birch,[55] F. C. R. Bishop,[49] A. Bitadze,[56] A. Bizzeti, M. P. Blago,[49] T. Blake,[50] F. Blanc,[43] J. E. Blank,[15] S. Blusk,[62] D. Bobulska,[53] J. A. Boelhauve,[15] O. Boente Garcia,[12] T. Boettcher,[59] A. Boldyrev,[38] C. S. Bolognani,[74] R. Bolzonella,[21,e] N. Bondar,[38,42] F. Borgato,[28] S. Borghi,[56] M. Borsato,[17] J. T. Borsuk,[35] S. A. Bouchiba,[43] T. J. V. Bowcock,[54] A. Boyer,[42] C. Bozzi,[21] M. J. Bradley,[55] S. Braun,[60] A. Brea Rodriguez,[40] J. Brodzicka,[35] A. Brossa Gonzalo,[40] J. Brown,[54] D. Brundu,[27] A. Buonaura,[44] L. Buonincontri,[28] A. T. Burke,[56] C. Burr,[42] A. Bursche,[66] A. Butkevich,[38] J. S. Butter,[32] J. Buytaert,[42] W. Byczynski,[42] S. Cadeddu,[27] H. Cai,[68] R. Calabrese,[21,e] L. Calefice,[15] S. Cali,[23] M. Calvi,[26,f] M. Calvo Gomez,[76] P. Campana,[23] D. H. Campora Perez,[74] A. F. Campoverde Quezada,[6] S. Capelli,[26,f] L. Capriotti,[20] A. Carbone,[20,g] R. Cardinale,[24,h] A. Cardini,[27] P. Carniti,[26,f] L. Carus,[14] A. Casais Vidal,[40] R. Caspary,[17] G. Casse,[54] M. Cattaneo,[42] G. Cavallero,[55,42] V. Cavallini,[21,e] S. Celani,[43] J. Cerasoli,[10] D. Cervenkov,[57] A. J. Chadwick,[54] I. Chahrour,[78] M. G. Chapman,[48] M. Charles,[13] Ph. Charpentier,[42] C. A. Chavez Barajas,[54] M. Chefdeville,[8] C. Chen,[10] S. Chen,[4] A. Chernov,[35] S. Chernyshenko,[46] V. Chobanova,[40] S. Cholak,[43] M. Chrzaszcz,[35] A. Chubykin,[38] V. Chulikov,[38] P. Ciambrone,[23] M. F. Cicala,[50] X. Cid Vidal,[40] G. Ciezarek,[42] P. Cifra,[42] G. Ciullo,[21,e] P. E. L. Clarke,[52] M. Clemencic,[42] H. V. Cliff,[49] J. Closier,[42] J. L. Cobbledick,[56] V. Coco,[42] J. A. B. Coelho,[11] J. Cogan,[10] E. Cogneras,[9] L. Cojocariu,[37] P. Collins,[42] T. Colombo,[42] L. Congedo,[19] A. Contu,[27] N. Cooke,[47] I. Corredoira,[40] G. Corti,[42] B. Couturier,[42] D. C. Craik,[44] M. Cruz Torres,[1,i] R. Currie,[52] C. L. Da Silva,[61] S. Dadabaev,[38] L. Dai,[65] X. Dai,[5] E. Dall'Occo,[15] J. Dalseno,[40] C. D'Ambrosio,[42] J. Daniel,[9] A. Danilina,[38] P. d'Argent,[19] J. E. Davies,[56] A. Davis,[56] O. De Aguiar Francisco,[56] J. de Boer,[42] K. De Bruyn,[73] S. De Capua,[56] M. De Cian,[43] U. De Freitas Carneiro Da Graca,[1] E. De Lucia,[23] J. M. De Miranda,[1] L. De Paula,[2] M. De Serio,[19,j] D. De Simone,[44] P. De Simone,[23] F. De Vellis,[15] J. A. de Vries,[74] C. T. Dean,[61] F. Debernardis,[19,j] D. Decamp,[8] V. Dedu,[10] L. Del Buono,[13] B. Delaney,[58] H.-P. Dembinski,[15] V. Denysenko,[44] O. Deschamps,[9] F. Dettori,[27,k] B. Dey,[71] P. Di Nezza,[23] I. Diachkov,[38] S. Didenko,[38] L. Dieste Maronas,[40] S. Ding,[62] V. Dobishuk,[46] A. Dolmatov,[38] C. Dong,[3] A. M. Donohoe,[18] F. Dordei,[27] A. C. dos Reis,[1] L. Douglas,[53] A. G. Downes,[8] P. Duda,[75] M. W. Dudek,[35] L. Dufour,[42] V. Duk,[72] P. Durante,[42] M. M. Duras,[75] J. M. Durham,[61] D. Dutta,[56] A. Dziurda,[35] A. Dzyuba,[38] S. Easo,[51] U. Egede,[63]

V. Egorychev,[38] C. Eirea Orro,[40] S. Eisenhardt,[52] E. Ejopu,[56] S. Ek-In,[43] L. Eklund,[77] M. E Elashri,[59] J. Ellbracht,[15] S. Ely,[55] A. Ene,[37] E. Epple,[59] S. Escher,[14] J. Eschle,[44] S. Esen,[44] T. Evans,[56] F. Fabiano,[27,k] L. N. Falcao,[1] Y. Fan,[6] B. Fang,[11,68] L. Fantini,[72,l] M. Faria,[43] S. Farry,[54] D. Fazzini,[26,f] L. F Felkowski,[75] M. Feo,[42] M. Fernandez Gomez,[40] A. D. Fernez,[60] F. Ferrari,[20] L. Ferreira Lopes,[43] F. Ferreira Rodrigues,[2] S. Ferreres Sole,[32] M. Ferrillo,[44] M. Ferro-Luzzi,[42] S. Filippov,[38] R. A. Fini,[19] M. Fiorini,[21,e] M. Firlej,[34] K. M. Fischer,[57] D. S. Fitzgerald,[78] C. Fitzpatrick,[56] T. Fiutowski,[34] F. Fleuret,[12] M. Fontana,[13] F. Fontanelli,[24,h] R. Forty,[42] D. Foulds-Holt,[49] V. Franco Lima,[54] M. Franco Sevilla,[60] M. Frank,[42] E. Franzoso,[21,e] G. Frau,[17] C. Frei,[42] D. A. Friday,[53] L. Frontini,[25] J. Fu,[6] Q. Fuehring,[15] T. Fulghesu,[13] E. Gabriel,[32] G. Galati,[19,j] M. D. Galati,[32] A. Gallas Torreira,[40] D. Galli,[20,g] S. Gambetta,[52,42] M. Gandelman,[2] P. Gandini,[25] Y. Gao,[7] Y. Gao,[5] M. Garau,[27,k] L. M. Garcia Martin,[50] P. Garcia Moreno,[39] J. García Pardiñas,[26,f] B. Garcia Plana,[40] F. A. Garcia Rosales,[12] L. Garrido,[39] C. Gaspar,[42] R. E. Geertsema,[32] D. Gerick,[17] L. L. Gerken,[15] E. Gersabeck,[56] M. Gersabeck,[56] T. Gershon,[50] L. Giambastiani,[28] V. Gibson,[49] H. K. Giemza,[36] A. L. Gilman,[57] M. Giovannetti,[23,b] A. Gioventù,[40] P. Gironella Gironell,[39] C. Giugliano,[21,e] M. A. Giza,[35] K. Gizdov,[52] E. L. Gkougkousis,[42] V. V. Gligorov,[13,42] C. Göbel,[64] E. Golobardes,[76] D. Golubkov,[38] A. Golutvin,[55,38] A. Gomes,[1,2,a,m,n] S. Gomez Fernandez,[39] F. Goncalves Abrantes,[57] M. Goncerz,[35] G. Gong,[3] I. V. Gorelov,[38] C. Gotti,[26] J. P. Grabowski,[70] T. Grammatico,[13] L. A. Granado Cardoso,[42] E. Graugés,[39] E. Graverini,[43] G. Graziani, A. T. Grecu,[37] L. M. Greeven,[32] N. A. Grieser,[59] L. Grillo,[53] S. Gromov,[38] B. R. Gruberg Cazon,[57] C. Gu,[3] M. Guarise,[21,e] M. Guittiere,[11] P. A. Günther,[17] E. Gushchin,[38] A. Guth,[14] Y. Guz,[38] T. Gys,[42] T. Hadavizadeh,[63] C. Hadjivasiliou,[60] G. Haefeli,[43] C. Haen,[42] J. Haimberger,[42] S. C. Haines,[49] T. Halewood-leagas,[54] M. M. Halvorsen,[42] P. M. Hamilton,[60] J. Hammerich,[54] Q. Han,[7] X. Han,[17] E. B. Hansen,[56] S. Hansmann-Menzemer,[17] L. Hao,[6] N. Harnew,[57] T. Harrison,[54] C. Hasse,[42] M. Hatch,[42] J. He,[6,o] K. Heijhoff,[32] F. H Hemmer,[42] C. Henderson,[59] R. D. L. Henderson,[63,50] A. M. Hennequin,[58] K. Hennessy,[54] L. Henry,[42] J. Herd,[55] J. Heuel,[14] A. Hicheur,[2] D. Hill,[43] M. Hilton,[56] S. E. Hollitt,[15] J. Horswill,[56] R. Hou,[7] Y. Hou,[8] J. Hu,[17] J. Hu,[66] W. Hu,[5] X. Hu,[3] W. Huang,[6] X. Huang,[68] W. Hulsbergen,[32] R. J. Hunter,[50] M. Hushchyn,[38] D. Hutchcroft,[54] P. Ibis,[15] M. Idzik,[34] D. Ilin,[38] P. Ilten,[59] A. Inglessi,[38] A. Iniukhin,[38] A. Ishteev,[38] K. Ivshin,[38] R. Jacobsson,[42] H. Jage,[14] S. J. Jaimes Elles,[41] S. Jakobsen,[42] E. Jans,[32] B. K. Jashal,[41] A. Jawahery,[60] V. Jevtic,[15] E. Jiang,[60] X. Jiang,[4,6] Y. Jiang,[6] M. John,[57] D. Johnson,[58] C. R. Jones,[49] T. P. Jones,[50] B. Jost,[42] N. Jurik,[42] I. Juszczak,[35] S. Kandybei,[45] Y. Kang,[3] M. Karacson,[42] D. Karpenkov,[38] M. Karpov,[38] J. W. Kautz,[59] F. Keizer,[42] D. M. Keller,[62] M. Kenzie,[50] T. Ketel,[32] B. Khanji,[15] A. Kharisova,[38] S. Kholodenko,[38] G. Khreich,[11] T. Kirn,[14] V. S. Kirsebom,[43] O. Kitouni,[58] S. Klaver,[33] N. Kleijne,[29,d] K. Klimaszewski,[36] M. R. Kmiec,[36] S. Koliiev,[46] L. Kolk,[15] A. Kondybayeva,[38] A. Konoplyannikov,[38] P. Kopciewicz,[34] R. Kopecna,[17] P. Koppenburg,[32] M. Korolev,[38] I. Kostiuk,[32] O. Kot,[46] S. Kotriakhova, A. Kozachuk,[38] P. Kravchenko,[38] L. Kravchuk,[38] R. D. Krawczyk,[42] M. Kreps,[50] S. Kretzschmar,[14] P. Krokovny,[38] W. Krupa,[34] W. Krzemien,[36] J. Kubat,[17] S. Kubis,[75] W. Kucewicz,[35] M. Kucharczyk,[35] V. Kudryavtsev,[38] E. K Kulikova,[38] A. Kupsc,[77] D. Lacarrere,[42] G. Lafferty,[56] A. Lai,[27] A. Lampis,[27,k] D. Lancierini,[44] C. Landesa Gomez,[40] J. J. Lane,[56] R. Lane,[48] C. Langenbruch,[14] J. Langer,[15] O. Lantwin,[38] T. Latham,[50] F. Lazzari,[29,p] M. Lazzaroni,[25,q] R. Le Gac,[10] S. H. Lee,[78] R. Lefèvre,[9] A. Leflat,[38] S. Legotin,[38] P. Lenisa,[21,e] O. Leroy,[10] T. Lesiak,[35] B. Leverington,[17] A. Li,[3] H. Li,[66] K. Li,[7] P. Li,[42] P.-R. Li,[67] S. Li,[7] T. Li,[4] T. Li,[66] Y. Li,[4] Z. Li,[62] X. Liang,[62] C. Lin,[6] T. Lin,[51] R. Lindner,[42] V. Lisovskyi,[15] R. Litvinov,[27,k] G. Liu,[66] H. Liu,[6] Q. Liu,[6] S. Liu,[4,6] A. Lobo Salvia,[39] A. Loi,[27] R. Lollini,[72] J. Lomba Castro,[40] I. Longstaff,[53] J. H. Lopes,[2] A. Lopez Huertas,[39] S. López Soliño,[40] G. H. Lovell,[49] Y. Lu,[4,r] C. Lucarelli,[22,c] D. Lucchesi,[28,s] S. Luchuk,[38] M. Lucio Martinez,[74] V. Lukashenko,[32,46] Y. Luo,[3] A. Lupato,[56] E. Luppi,[21,e] A. Lusiani,[29,d] K. Lynch,[18] X.-R. Lyu,[6] R. Ma,[6] S. Maccolini,[15] F. Machefert,[11] F. Maciuc,[37] I. Mackay,[57] V. Macko,[43] L. R. Madhan Mohan,[48] A. Maevskiy,[38] D. Maisuzenko,[38] M. W. Majewski,[34] J. J. Malczewski,[35] S. Malde,[57] B. Malecki,[35,42] A. Malinin,[38] T. Maltsev,[38] G. Manca,[27,k] G. Mancinelli,[10] C. Mancuso,[11,25,q] R. Manera Escalero,[39] D. Manuzzi,[20] C. A. Manzari,[44] D. Marangotto,[25,q] J. F. Marchand,[8] U. Marconi,[20] S. Mariani,[22,c] C. Marin Benito,[39] J. Marks,[17] A. M. Marshall,[48] P. J. Marshall,[54] G. Martelli,[72,l] G. Martellotti,[30] L. Martinazzoli,[42,f] M. Martinelli,[26,f] D. Martinez Santos,[40] F. Martinez Vidal,[41] A. Massafferri,[1] M. Materok,[14] R. Matev,[42] A. Mathad,[44]

V. Matiunin,[38] C. Matteuzzi,[26] K. R. Mattioli,[12] A. Mauri,[32] E. Maurice,[12] J. Mauricio,[39] M. Mazurek,[42] M. McCann,[55] L. Mcconnell,[18] T. H. McGrath,[56] N. T. McHugh,[53] A. McNab,[56] R. McNulty,[18] J. V. Mead,[54] B. Meadows,[59] G. Meier,[15] D. Melnychuk,[36] S. Meloni,[26,f] M. Merk,[32,74] A. Merli,[25,q] L. Meyer Garcia,[2] D. Miao,[4,6] M. Mikhasenko,[70,t] D. A. Milanes,[69] E. Millard,[50] M. Milovanovic,[42] M.-N. Minard,[8,a] A. Minotti,[26,f] T. Miralles,[9] S. E. Mitchell,[52] B. Mitreska,[15] D. S. Mitzel,[15] A. Mödden,[15] R. A. Mohammed,[57] R. D. Moise,[14] S. Mokhnenko,[38] T. Mombächer,[40] M. Monk,[50,63] I. A. Monroy,[69] S. Monteil,[9] G. Morello,[23] M. J. Morello,[29,d] M. P. Morgenthaler,[17] J. Moron,[34] A. B. Morris,[42] A. G. Morris,[50] R. Mountain,[62] H. Mu,[3] E. Muhammad,[50] F. Muheim,[52] M. Mulder,[73] K. Müller,[44] C. H. Murphy,[57] D. Murray,[56] R. Murta,[55] P. Muzzetto,[27,k] P. Naik,[48] T. Nakada,[43] R. Nandakumar,[51] T. Nanut,[42] I. Nasteva,[2] M. Needham,[52] N. Neri,[25,q] S. Neubert,[70] N. Neufeld,[42] P. Neustroev,[38] R. Newcombe,[55] J. Nicolini,[15,11] D. Nicotra,[74] E. M. Niel,[43] S. Nieswand,[14] N. Nikitin,[38] N. S. Nolte,[58] C. Normand,[8,27,k] J. Novoa Fernandez,[40] G. N Nowak,[59] C. Nunez,[78] A. Oblakowska-Mucha,[34] V. Obraztsov,[38] T. Oeser,[14] S. Okamura,[21,e] R. Oldeman,[27,k] F. Oliva,[52] C. J. G. Onderwater,[73] R. H. O'Neil,[52] J. M. Otalora Goicochea,[2] T. Ovsiannikova,[38] P. Owen,[44] A. Oyanguren,[41] O. Ozcelik,[52] K. O. Padeken,[70] B. Pagare,[50] P. R. Pais,[42] T. Pajero,[57] A. Palano,[19] M. Palutan,[23] Y. Pan,[56] G. Panshin,[38] L. Paolucci,[50] A. Papanestis,[51] M. Pappagallo,[19,j] L. L. Pappalardo,[21,e] C. Pappenheimer,[59] W. Parker,[60] C. Parkes,[56] B. Passalacqua,[21,e] G. Passaleva,[22] A. Pastore,[19] M. Patel,[55] C. Patrignani,[20,g] C. J. Pawley,[74] A. Pellegrino,[32] M. Pepe Altarelli,[42] S. Perazzini,[20] D. Pereima,[38] A. Pereiro Castro,[40] P. Perret,[9] K. Petridis,[48] A. Petrolini,[24,h] A. Petrov,[38] S. Petrucci,[52] M. Petruzzo,[25] H. Pham,[62] A. Philippov,[38] R. Piandani,[6] L. Pica,[29,d] M. Piccini,[72] B. Pietrzyk,[8] G. Pietrzyk,[11] M. Pili,[57] D. Pinci,[30] F. Pisani,[42] M. Pizzichemi,[26,42,f] V. Placinta,[37] J. Plews,[47] M. Plo Casasus,[40] F. Polci,[13,42] M. Poli Lener,[23] A. Poluektov,[10] N. Polukhina,[38] I. Polyakov,[42] E. Polycarpo,[2] S. Ponce,[42] D. Popov,[6,42] S. Poslavskii,[38] K. Prasanth,[35] L. Promberger,[17] C. Prouve,[40] V. Pugatch,[46] V. Puill,[11] G. Punzi,[29,p] H. R. Qi,[3] W. Qian,[6] N. Qin,[3] S. Qu,[3] R. Quagliani,[43] N. V. Raab,[18] B. Rachwal,[34] J. H. Rademacker,[48] R. Rajagopalan,[62] M. Rama,[29] M. Ramos Pernas,[50] M. S. Rangel,[2] F. Ratnikov,[38] G. Raven,[33,42] M. Rebollo De Miguel,[41] F. Redi,[42] J. Reich,[48] F. Reiss,[56] C. Remon Alepuz,[41] Z. Ren,[3] P. K. Resmi,[57] R. Ribatti,[29,d] A. M. Ricci,[27] S. Ricciardi,[51] K. Richardson,[58] M. Richardson-Slipper,[52] K. Rinnert,[54] P. Robbe,[11] G. Robertson,[52] A. B. Rodrigues,[43] E. Rodrigues,[54] E. Rodriguez Fernandez,[40] J. A. Rodriguez Lopez,[69] E. Rodriguez Rodriguez,[40] D. L. Rolf,[42] A. Rollings,[57] P. Roloff,[42] V. Romanovskiy,[38] M. Romero Lamas,[40] A. Romero Vidal,[40] J. D. Roth,[78,a] M. Rotondo,[23] M. S. Rudolph,[62] T. Ruf,[42] R. A. Ruiz Fernandez,[40] J. Ruiz Vidal,[41] A. Ryzhikov,[38] J. Ryzka,[34] J. J. Saborido Silva,[40] N. Sagidova,[38] N. Sahoo,[47] B. Saitta,[27,k] M. Salomoni,[42] C. Sanchez Gras,[32] I. Sanderswood,[41] R. Santacesaria,[30] C. Santamarina Rios,[40] M. Santimaria,[23] E. Santovetti,[31,b] D. Saranin,[38] G. Sarpis,[14] M. Sarpis,[70] A. Sarti,[30] C. Satriano,[30,u] A. Satta,[31] M. Saur,[15] D. Savrina,[38] H. Sazak,[9] L. G. Scantlebury Smead,[57] A. Scarabotto,[13] S. Schael,[14] S. Scherl,[54] M. Schiller,[53] H. Schindler,[42] M. Schmelling,[16] B. Schmidt,[42] S. Schmitt,[14] O. Schneider,[43] A. Schopper,[42] M. Schubiger,[32] S. Schulte,[43] M. H. Schune,[11] R. Schwemmer,[42] B. Sciascia,[23] A. Sciuccati,[42] S. Sellam,[40] A. Semennikov,[38] M. Senghi Soares,[33] A. Sergi,[24,h] N. Serra,[44] L. Sestini,[28] A. Seuthe,[15] Y. Shang,[5] D. M. Shangase,[78] M. Shapkin,[38] I. Shchemerov,[38] L. Shchutska,[43] T. Shears,[54] L. Shekhtman,[38] Z. Shen,[5] S. Sheng,[4,6] V. Shevchenko,[38] B. Shi,[6] E. B. Shields,[26,f] Y. Shimizu,[11] E. Shmanin,[38] R. Shorkin,[38] J. D. Shupperd,[62] B. G. Siddi,[21,e] R. Silva Coutinho,[62] G. Simi,[28] S. Simone,[19,j] M. Singla,[63] N. Skidmore,[56] R. Skuza,[17] T. Skwarnicki,[62] M. W. Slater,[47] J. C. Smallwood,[57] J. G. Smeaton,[49] E. Smith,[44] K. Smith,[61] M. Smith,[55] A. Snoch,[32] L. Soares Lavra,[9] M. D. Sokoloff,[59] F. J. P. Soler,[53] A. Solomin,[38,48] A. Solovev,[38] I. Solovyev,[38] R. Song,[63] F. L. Souza De Almeida,[2] B. Souza De Paula,[2] B. Spaan,[15,a] E. Spadaro Norella,[25,q] E. Spedicato,[20] E. Spiridenkov,[38] P. Spradlin,[53] V. Sriskaran,[42] F. Stagni,[42] M. Stahl,[42] S. Stahl,[42] S. Stanislaus,[57] E. N. Stein,[42] O. Steinkamp,[44] O. Stenyakin,[38] H. Stevens,[15] S. Stone,[62,a] D. Strekalina,[38] Y. S Su,[6] F. Suljik,[57] J. Sun,[27] L. Sun,[68] Y. Sun,[60] P. Svihra,[56] P. N. Swallow,[47] K. Swientek,[34] A. Szabelski,[36] T. Szumlak,[34] M. Szymanski,[42] Y. Tan,[3] S. Taneja,[56] M. D. Tat,[57] A. Terentev,[44] F. Teubert,[42] E. Thomas,[42] D. J. D. Thompson,[47] K. A. Thomson,[54] H. Tilquin,[55] V. Tisserand,[9] S. T'Jampens,[8] M. Tobin,[4] L. Tomassetti,[21,e] G. Tonani,[25,q] X. Tong,[5] D. Torres Machado,[1] D. Y. Tou,[3] S. M. Trilov,[48] C. Trippl,[43] G. Tuci,[6] N. Tuning,[32] A. Ukleja,[36] D. J. Unverzagt,[17] A. Usachov,[33] A. Ustyuzhanin,[38] U. Uwer,[17]

A. Vagner,[38] V. Vagnoni,[20] A. Valassi,[42] G. Valenti,[20] N. Valls Canudas,[76] M. Van Dijk,[43] H. Van Hecke,[61] E. van Herwijnen,[55] C. B. Van Hulse,[40,v] M. van Veghel,[32] R. Vazquez Gomez,[39] P. Vazquez Regueiro,[40] C. Vázquez Sierra,[42] S. Vecchi,[21] J. J. Velthuis,[48] M. Veltri,[22,w] A. Venkateswaran,[43] M. Veronesi,[32] M. Vesterinen,[50] D. Vieira,[59] M. Vieites Diaz,[43] X. Vilasis-Cardona,[76] E. Vilella Figueras,[54] A. Villa,[20] P. Vincent,[13] F. C. Volle,[11] D. vom Bruch,[10] A. Vorobyev,[38] V. Vorobyev,[38] N. Voropaev,[38] K. Vos,[74] C. Vrahas,[52] J. Walsh,[29] E. J. Walton,[63] G. Wan,[5] C. Wang,[17] G. Wang,[7] J. Wang,[5] J. Wang,[4] J. Wang,[3] J. Wang,[68] M. Wang,[25] R. Wang,[48] X. Wang,[66] Y. Wang,[7] Z. Wang,[44] Z. Wang,[3] Z. Wang,[6] J. A. Ward,[50,63] N. K. Watson,[47] D. Websdale,[55] Y. Wei,[5] B. D. C. Westhenry,[48] D. J. White,[56] M. Whitehead,[53] A. R. Wiederhold,[50] D. Wiedner,[15] G. Wilkinson,[57] M. K. Wilkinson,[59] I. Williams,[49] M. Williams,[58] M. R. J. Williams,[52] R. Williams,[49] F. F. Wilson,[51] W. Wislicki,[36] M. Witek,[35] L. Witola,[17] C. P. Wong,[61] G. Wormser,[11] S. A. Wotton,[49] H. Wu,[62] J. Wu,[7] K. Wyllie,[42] Z. Xiang,[6] Y. Xie,[7] A. Xu,[5] J. Xu,[6] L. Xu,[3] L. Xu,[3] M. Xu,[50] Q. Xu,[6] Z. Xu,[9] Z. Xu,[6] D. Yang,[3] S. Yang,[6] X. Yang,[5] Y. Yang,[6] Z. Yang,[5] Z. Yang,[60] L. E. Yeomans,[54] V. Yeroshenko,[11] H. Yeung,[56] H. Yin,[7] J. Yu,[65] X. Yuan,[62] E. Zaffaroni,[43] M. Zavertyaev,[16] M. Zdybal,[35] M. Zeng,[3] C. Zhang,[5] D. Zhang,[7] L. Zhang,[3] S. Zhang,[65] S. Zhang,[5] Y. Zhang,[5] Y. Zhang,[57] Y. Zhao,[17] A. Zharkova,[38] A. Zhelezov,[17] Y. Zheng,[6] T. Zhou,[5] X. Zhou,[6] Y. Zhou,[6] V. Zhovkovska,[11] X. Zhu,[3] X. Zhu,[7] Z. Zhu,[6] V. Zhukov,[14,38] Q. Zou,[4,6] S. Zucchelli,[20,g] D. Zuliani,[28] and G. Zunica[56]

(LHCb Collaboration)

[1]*Centro Brasileiro de Pesquisas Físicas (CBPF), Rio de Janeiro, Brazil*
[2]*Universidade Federal do Rio de Janeiro (UFRJ), Rio de Janeiro, Brazil*
[3]*Center for High Energy Physics, Tsinghua University, Beijing, China*
[4]*Institute of High Energy Physics (IHEP), Beijing, China*
[5]*School of Physics State Key Laboratory of Nuclear Physics and Technology, Peking University, Beijing, China*
[6]*University of Chinese Academy of Sciences, Beijing, China*
[7]*Institute of Particle Physics, Central China Normal University, Wuhan, Hubei, China*
[8]*Université Savoie Mont Blanc, CNRS, IN2P3-LAPP, Annecy, France*
[9]*Université Clermont Auvergne, CNRS/IN2P3, LPC, Clermont-Ferrand, France*
[10]*Aix Marseille Université, CNRS/IN2P3, CPPM, Marseille, France*
[11]*Université Paris-Saclay, CNRS/IN2P3, IJCLab, Orsay, France*
[12]*Laboratoire Leprince-Ringuet, CNRS/IN2P3, Ecole Polytechnique, Institut Polytechnique de Paris, Palaiseau, France*
[13]*LPNHE, Sorbonne Université, Paris Diderot Sorbonne Paris Cité, CNRS/IN2P3, Paris, France*
[14]*I. Physikalisches Institut, RWTH Aachen University, Aachen, Germany*
[15]*Fakultät Physik, Technische Universität Dortmund, Dortmund, Germany*
[16]*Max-Planck-Institut für Kernphysik (MPIK), Heidelberg, Germany*
[17]*Physikalisches Institut, Ruprecht-Karls-Universität Heidelberg, Heidelberg, Germany*
[18]*School of Physics, University College Dublin, Dublin, Ireland*
[19]*INFN Sezione di Bari, Bari, Italy*
[20]*INFN Sezione di Bologna, Bologna, Italy*
[21]*INFN Sezione di Ferrara, Ferrara, Italy*
[22]*INFN Sezione di Firenze, Firenze, Italy*
[23]*INFN Laboratori Nazionali di Frascati, Frascati, Italy*
[24]*INFN Sezione di Genova, Genova, Italy*
[25]*INFN Sezione di Milano, Milano, Italy*
[26]*INFN Sezione di Milano-Bicocca, Milano, Italy*
[27]*INFN Sezione di Cagliari, Monserrato, Italy*
[28]*Università degli Studi di Padova, Università e INFN, Padova, Padova, Italy*
[29]*INFN Sezione di Pisa, Pisa, Italy*
[30]*INFN Sezione di Roma La Sapienza, Roma, Italy*
[31]*INFN Sezione di Roma Tor Vergata, Roma, Italy*
[32]*Nikhef National Institute for Subatomic Physics, Amsterdam, Netherlands*
[33]*Nikhef National Institute for Subatomic Physics and VU University Amsterdam, Amsterdam, Netherlands*
[34]*AGH - University of Science and Technology, Faculty of Physics and Applied Computer Science, Kraków, Poland*
[35]*Henryk Niewodniczanski Institute of Nuclear Physics Polish Academy of Sciences, Kraków, Poland*
[36]*National Center for Nuclear Research (NCBJ), Warsaw, Poland*

[37]Horia Hulubei National Institute of Physics and Nuclear Engineering, Bucharest-Magurele, Romania
[38]Affiliated with an institute covered by a cooperation agreement with CERN
[39]ICCUB, Universitat de Barcelona, Barcelona, Spain
[40]Instituto Galego de Física de Altas Enerxías (IGFAE), Universidade de Santiago de Compostela, Santiago de Compostela, Spain
[41]Instituto de Fisica Corpuscular, Centro Mixto Universidad de Valencia - CSIC, Valencia, Spain
[42]European Organization for Nuclear Research (CERN), Geneva, Switzerland
[43]Institute of Physics, Ecole Polytechnique Fédérale de Lausanne (EPFL), Lausanne, Switzerland
[44]Physik-Institut, Universität Zürich, Zürich, Switzerland
[45]NSC Kharkiv Institute of Physics and Technology (NSC KIPT), Kharkiv, Ukraine
[46]Institute for Nuclear Research of the National Academy of Sciences (KINR), Kyiv, Ukraine
[47]University of Birmingham, Birmingham, United Kingdom
[48]H.H. Wills Physics Laboratory, University of Bristol, Bristol, United Kingdom
[49]Cavendish Laboratory, University of Cambridge, Cambridge, United Kingdom
[50]Department of Physics, University of Warwick, Coventry, United Kingdom
[51]STFC Rutherford Appleton Laboratory, Didcot, United Kingdom
[52]School of Physics and Astronomy, University of Edinburgh, Edinburgh, United Kingdom
[53]School of Physics and Astronomy, University of Glasgow, Glasgow, United Kingdom
[54]Oliver Lodge Laboratory, University of Liverpool, Liverpool, United Kingdom
[55]Imperial College London, London, United Kingdom
[56]Department of Physics and Astronomy, University of Manchester, Manchester, United Kingdom
[57]Department of Physics, University of Oxford, Oxford, United Kingdom
[58]Massachusetts Institute of Technology, Cambridge, 02139 Massachusetts, USA
[59]University of Cincinnati, Cincinnati, 45221 Ohio, USA
[60]University of Maryland, College Park, 20742 Maryland, USA
[61]Los Alamos National Laboratory (LANL), Los Alamos, 87545 New Mexico, USA
[62]Syracuse University, Syracuse, 13244 New York, USA
[63]School of Physics and Astronomy, Monash University, Melbourne, Australia
(associated with Department of Physics, University of Warwick, Coventry, United Kingdom)
[64]Pontifícia Universidade Católica do Rio de Janeiro (PUC-Rio), Rio de Janeiro, Brazil
(associated with Universidade Federal do Rio de Janeiro (UFRJ), Rio de Janeiro, Brazil)
[65]Physics and Micro Electronic College, Hunan University, Changsha City, China
(associated with Institute of Particle Physics, Central China Normal University, Wuhan, Hubei, China)
[66]Guangdong Provincial Key Laboratory of Nuclear Science, Guangdong-Hong Kong Joint Laboratory of Quantum Matter, Institute of Quantum Matter, South China Normal University, Guangzhou, China
(associated with Center for High Energy Physics, Tsinghua University, Beijing, China)
[67]Lanzhou University, Lanzhou, China
(associated with Institute Of High Energy Physics (IHEP), Beijing, China)
[68]School of Physics and Technology, Wuhan University, Wuhan, China
(associated with Center for High Energy Physics, Tsinghua University, Beijing, China)
[69]Departamento de Fisica, Universidad Nacional de Colombia, Bogota, Colombia
(associated with LPNHE, Sorbonne Université, Paris Diderot Sorbonne Paris Cité, CNRS/IN2P3, Paris, France)
[70]Universität Bonn - Helmholtz-Institut für Strahlen und Kernphysik, Bonn, Germany
(associated with Physikalisches Institut, Ruprecht-Karls-Universität Heidelberg, Heidelberg, Germany)
[71]Eotvos Lorand University, Budapest, Hungary
(associated with European Organization for Nuclear Research (CERN), Geneva, Switzerland)
[72]INFN Sezione di Perugia, Perugia, Italy
(associated with INFN Sezione di Ferrara, Ferrara, Italy)
[73]Van Swinderen Institute, University of Groningen, Groningen, Netherlands
(associated with Nikhef National Institute for Subatomic Physics, Amsterdam, Netherlands)
[74]Universiteit Maastricht, Maastricht, Netherlands
(associated with Nikhef National Institute for Subatomic Physics, Amsterdam, Netherlands)
[75]Tadeusz Kosciuszko Cracow University of Technology, Cracow, Poland
(associated with Henryk Niewodniczanski Institute of Nuclear Physics Polish Academy of Sciences, Kraków, Poland)
[76]DS4DS, La Salle, Universitat Ramon Llull, Barcelona, Spain
(associated with ICCUB, Universitat de Barcelona, Barcelona, Spain)
[77]Department of Physics and Astronomy, Uppsala University, Uppsala, Sweden
(associated with School of Physics and Astronomy, University of Glasgow, Glasgow, United Kingdom)
[78]University of Michigan, Ann Arbor, 48109 Michigan, USA
(associated with Syracuse University, Syracuse, New York, USA)

[a]Deceased.
[b]Also at Università di Roma Tor Vergata, Roma, Italy.
[c]Also at Università di Firenze, Firenze, Italy.
[d]Also at Scuola Normale Superiore, Pisa, Italy.
[e]Also at Università di Ferrara, Ferrara, Italy.
[f]Also at Università di Milano Bicocca, Milano, Italy.
[g]Also at Università di Bologna, Bologna, Italy.
[h]Also at Università di Genova, Genova, Italy.
[i]Also at Universidad Nacional Autónoma de Honduras, Tegucigalpa, Honduras.
[j]Also at Università di Bari, Bari, Italy.
[k]Also at Università di Cagliari, Cagliari, Italy.
[l]Also at Università di Perugia, Perugia, Italy.
[m]Also at Universidade Federal do Triângulo Mineiro (UFTM), Uberaba-MG, Brazil.
[n]Also at Universidade de Brasília, Brasília, Brazil.
[o]Also at Hangzhou Institute for Advanced Study, UCAS, Hangzhou, China.
[p]Also at Università di Pisa, Pisa, Italy.
[q]Also at Università degli Studi di Milano, Milano, Italy.
[r]Also at Central South University, Changsha, China.
[s]Also at Università di Padova, Padova, Italy.
[t]Also at Excellence Cluster ORIGINS, Munich, Germany.
[u]Also at Università della Basilicata, Potenza, Italy.
[v]Also at Universidad de Alcalá, Alcalá de Henares, Spain.
[w]Also at Università di Urbino, Urbino, Italy.